Mechanisms of Strontium and Uranium Removal from High-level Radioactive Waste Simulant Solutions by the Sorbent Monosodium Titanate

M. C. Duff [1,*], D. B. Hunter [1], D. T. Hobbs [1], S. D. Fink [1], Z. Dai [2,3], and J. P. Bradley [2,3]

---

[1] Westinghouse Savannah River Company (WSRC), Savannah River National Laboratory (SRNL), Aiken, SC 29808, USA.

* Corresponding author, SRNL, Bldg. 773-43A, Rm. 217, Aiken, SC 29808, USA. phone: (803) 725-2054; fax: (803) 725-4704; e-mail: martine.duff@srs.gov

[2] MVA Incorporated, 5500 Oakbrook Parkway, Norcross, GA, 30093, USA.

[3] Presently with Lawrence Livermore National Laboratory, Livermore, CA, 94551, USA.

Number of Pages: 9

Number of Figures: 13

Number of Tables: none

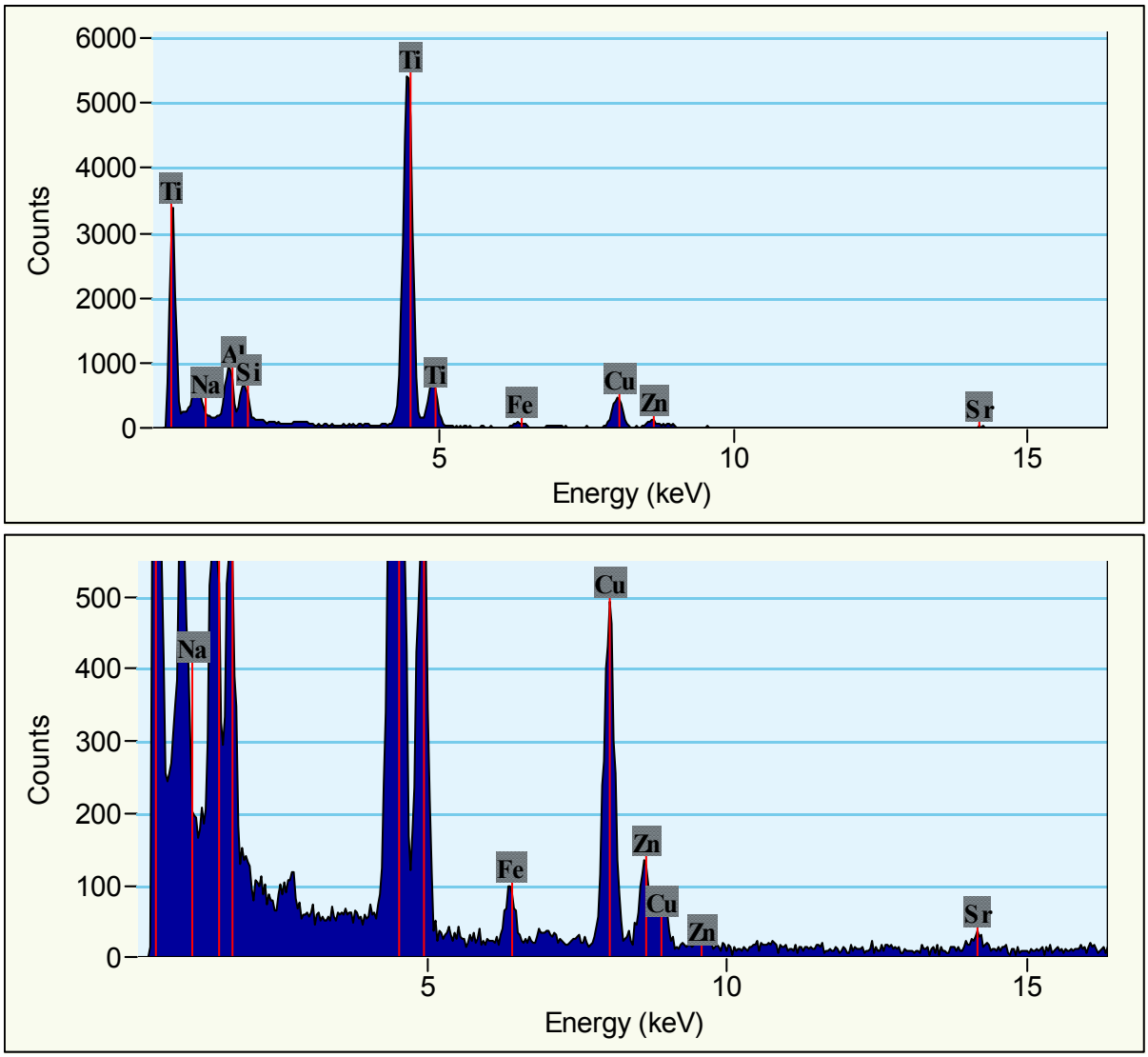

Sr-MST1 Edge area

Supplemental Figure 1. EDS spectra taken on the fringe edges of the Sr-loaded MST showing the presence of small amounts of Sr, in addition to larger amounts of Ti, Al, Na, Si, Fe and Zn (the Cu peaks are from the Cu in the sample grid).

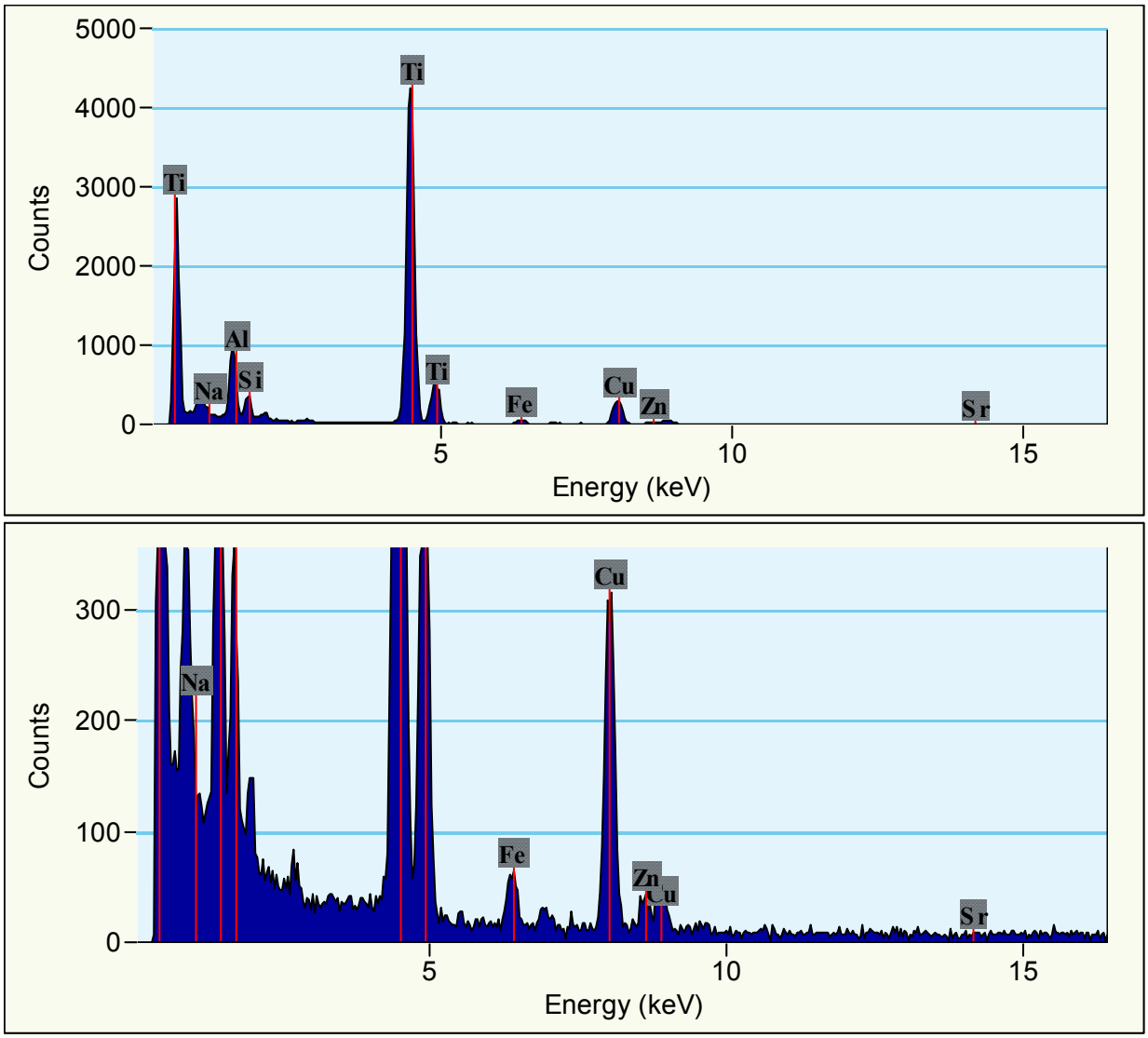

Sr-MST1 Center area

Supplemental Figure 2. EDS spectra taken on the internal (amorphous) regions of the Sr-loaded MST showing the absence of Sr and the presence of Ti, Al, Na, Si, Fe and Zn (the Cu peaks are from the Cu in the sample grid).

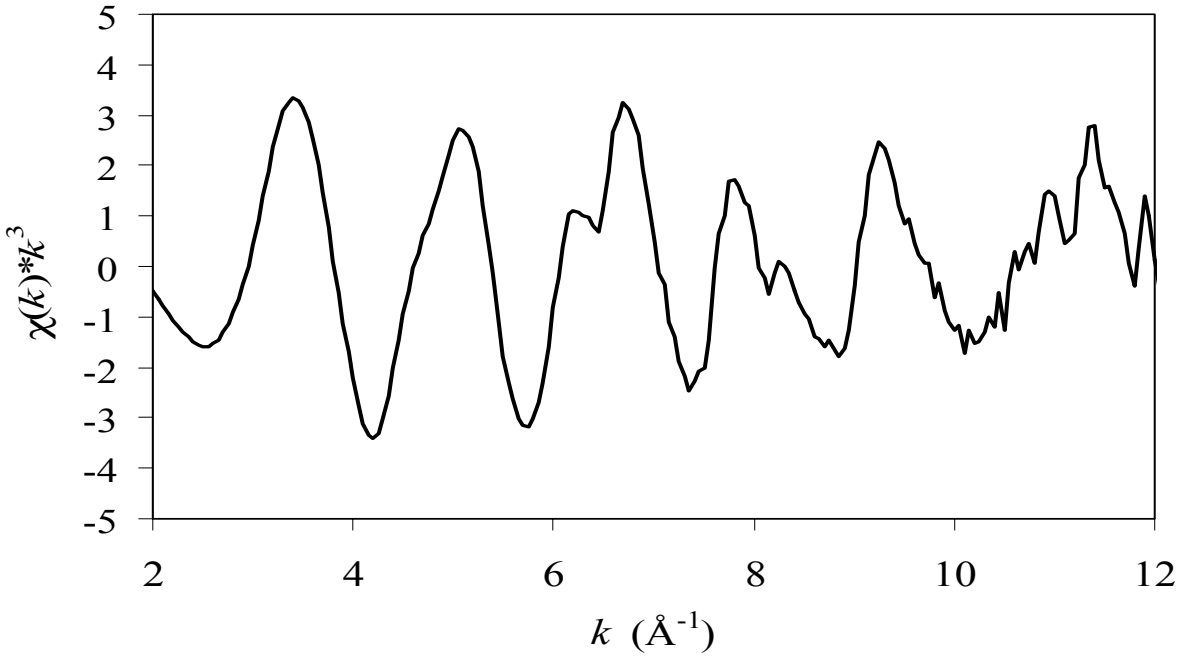

Supplemental Figure 3. The k^3-weighted chi data for aqueous Sr^{2+} in a HLW stimulant solution.

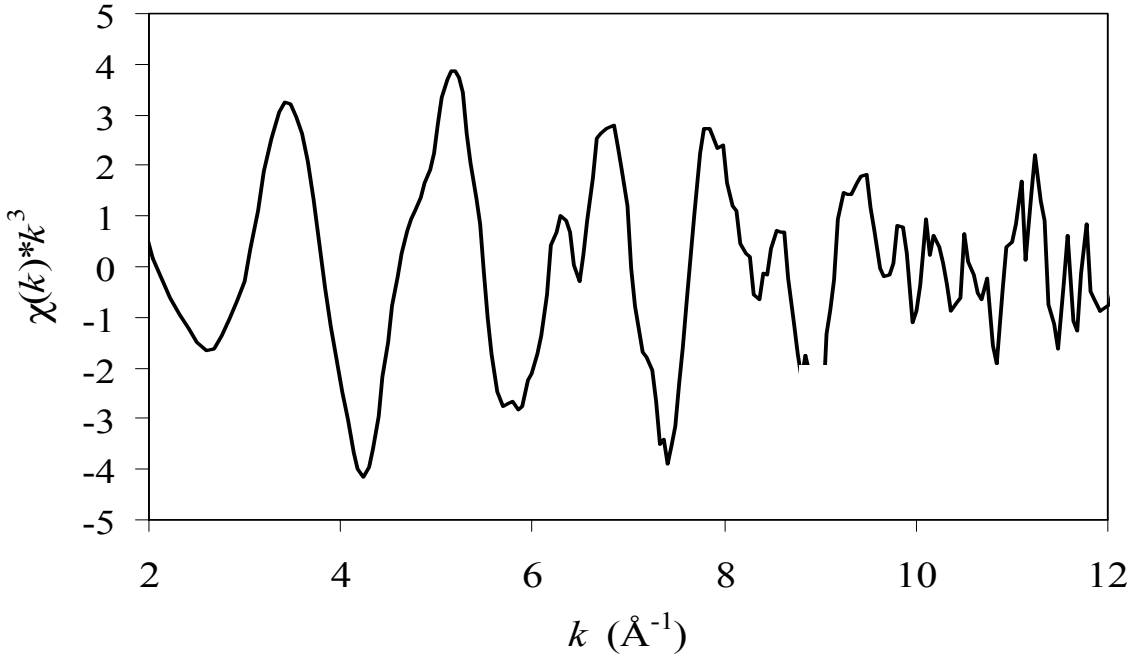

Supplemental Figure 4. The k^3-weighted chi data for Sr^{2+} in $SrCO_{3(s)}$.

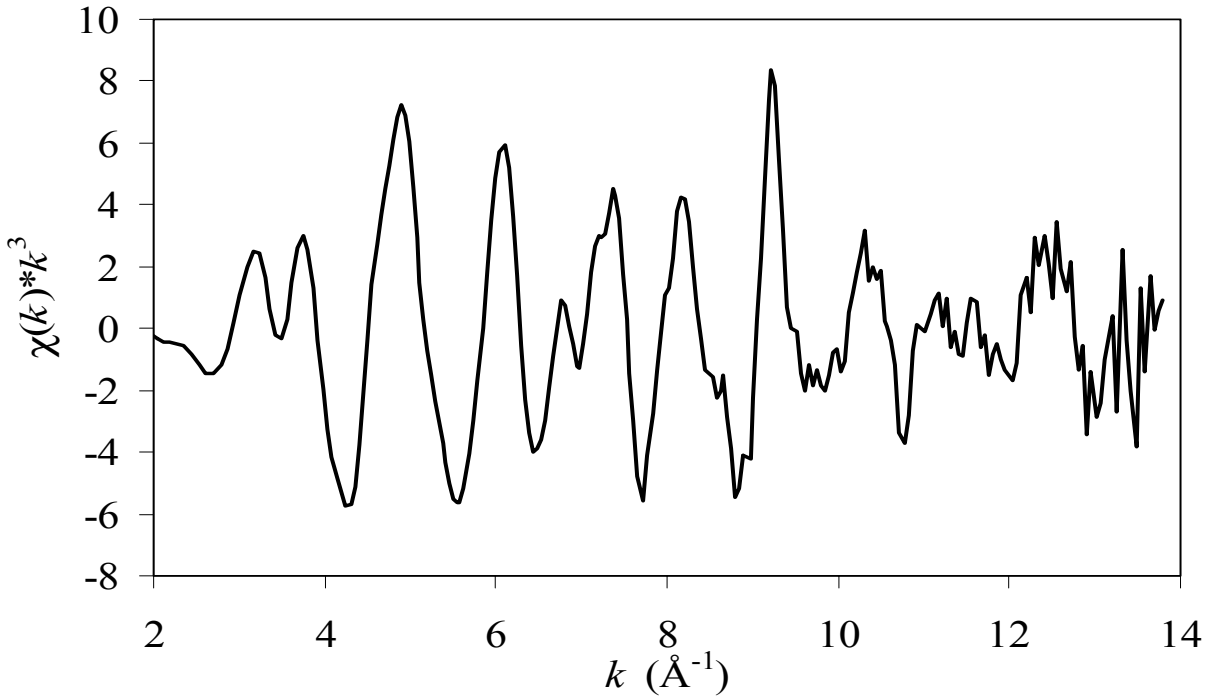

Supplemental Figure 5. The k^3-weighted chi data for Sr^{2+} in $SrTiO_{3(s)}$.

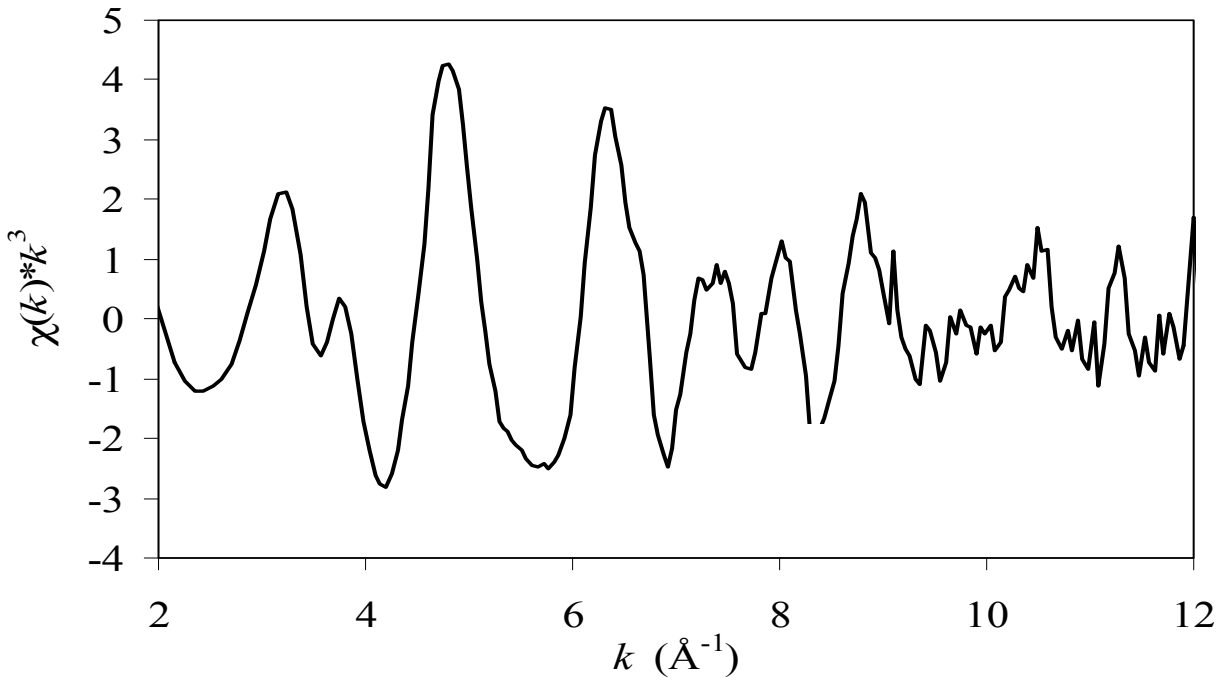

Supplemental Figure 6. The k^3-weighted chi data for Sr^{2+} in $Sr(NO_3)_{2(s)}$.

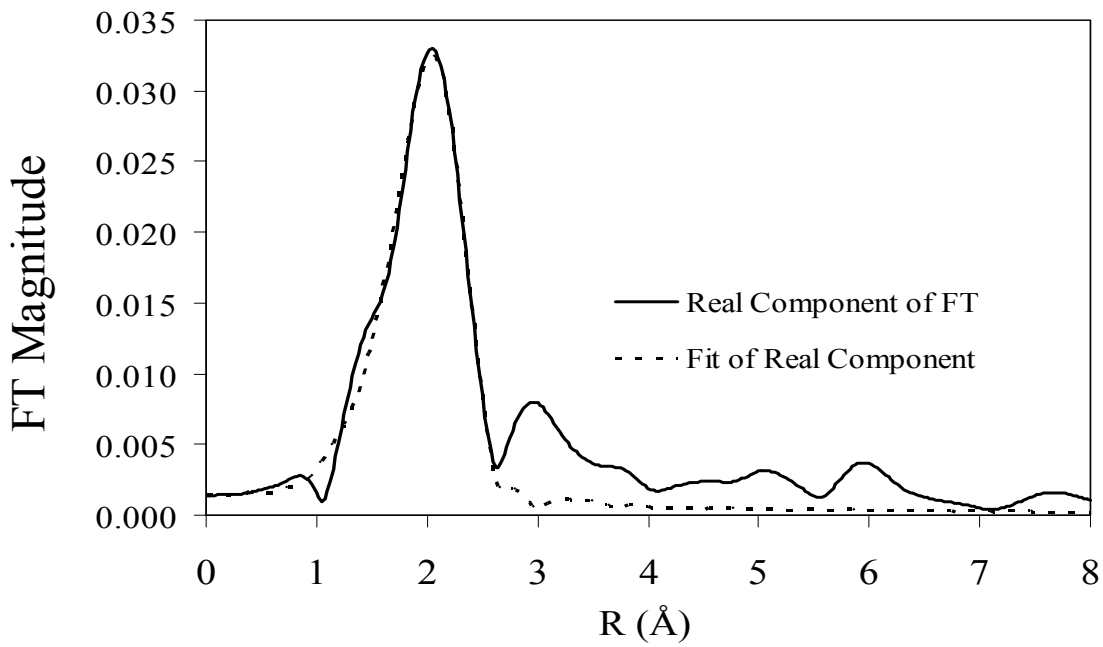

Supplemental Figure 7. FT data for SrMST1 showing the fit for O using the third cumulant—uncorrected for phase shift.

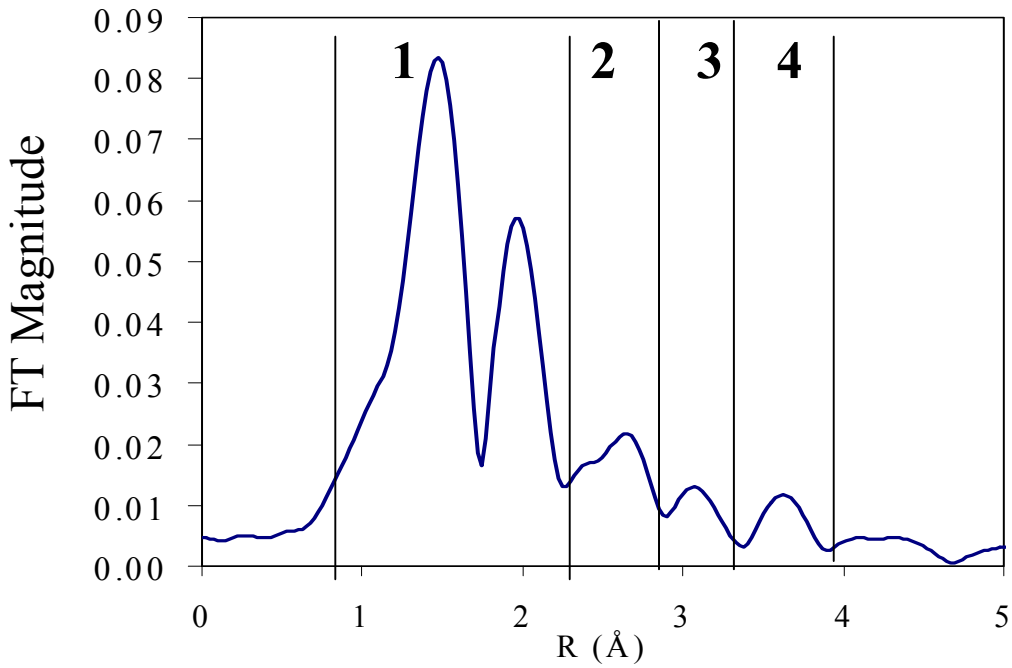

Supplemental Figure 8. FT data for UMST1 showing the approximate regions that were selected for back transforms and fits in chi space—uncorrected for phase shift.

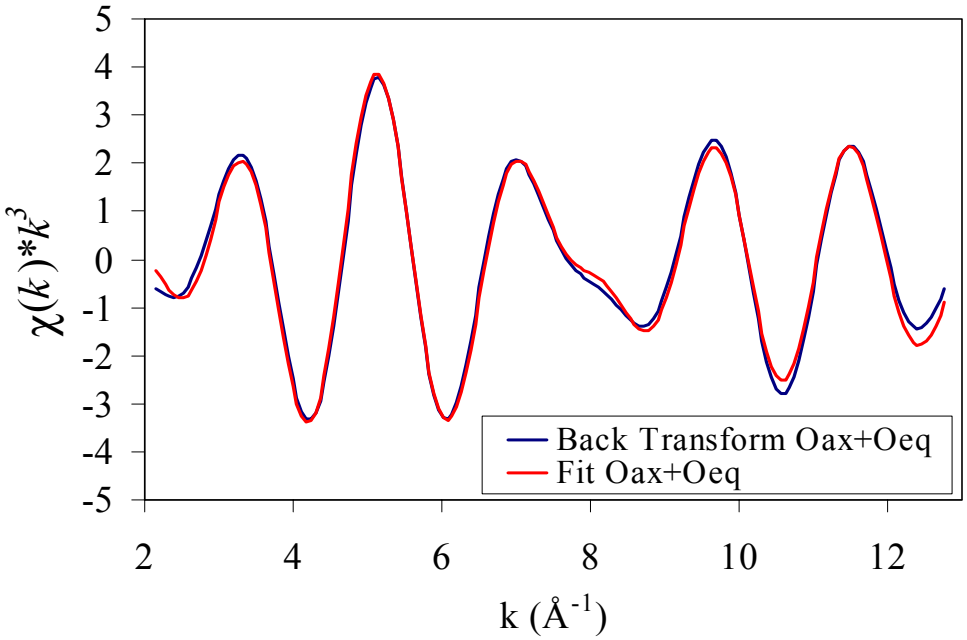

Supplemental Figure 9. Fourier-filtered XAFS data for R-space region 1 of the FT data for UMST1 and corresponding model fit data**.**

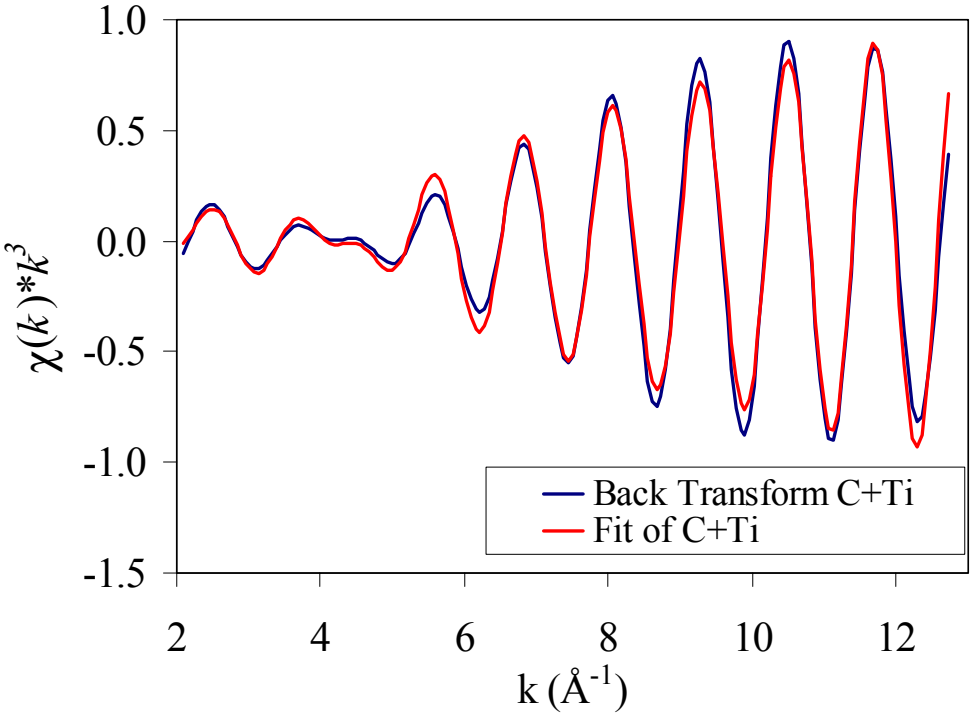

Supplemental Figure 10. Fourier-filtered XAFS data for R-space region 3 of the FT data for UMST1 and corresponding model fit data**.**

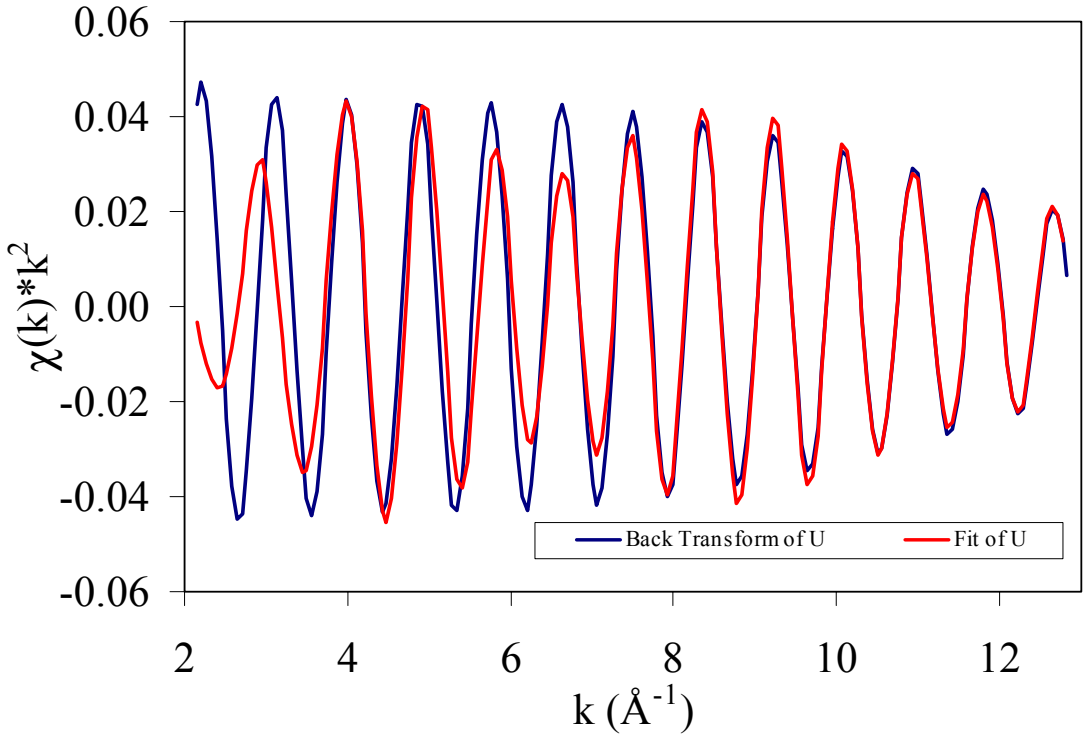

Supplemental Figure 11. Fourier-filtered XAFS data for R-space region 4 of the FT data for UMST1 and corresponding model fit data**.**

Short U-Ti Distance

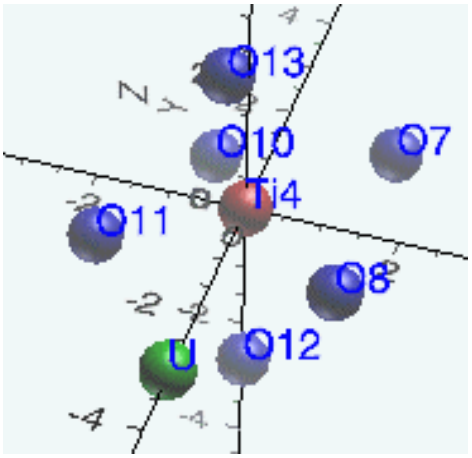

Ti(4) Distorted Octahedron
Bond Angle O11-Ti4-O8= 105.61°
Fixed Bond Lengths:
Ti4-O11 = 1.98 Å
Ti4-O8 = 1.90 Å
U-O11 = 2.40 Å
U-O8 = 2.40 Å
Resultant Radial Distance:
U-Ti4 = 3.00 Å

Supplemental Figure 12. Molecular modeling simulations of U associating with a distorted Ti octahedron called Ti(4) via specific adsorption. The image demonstrates a short U-Ti radial distance of 3 Å is realistic.

Long U-Ti Distance

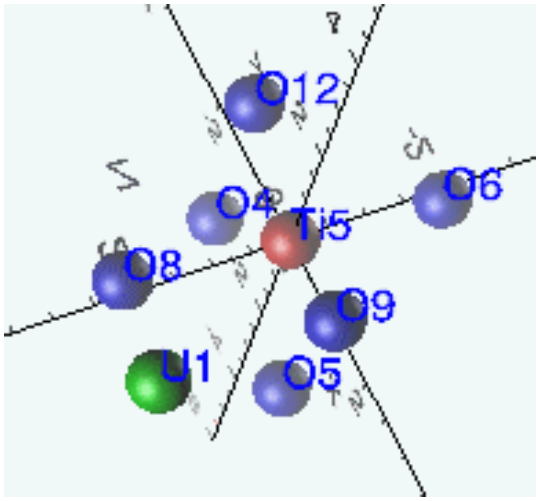

Ti(5) Distorted Octahedron
Bond Angle O8-Ti5-O9= 71.0°
Fixed Bond Lengths:
Ti5-O8 = 2.23 Å
Ti5-O9 = 2.09 Å
U-O8 = 2.40 Å
U-O9 = 2.40 Å
Resultant Radial Distance:
U-Ti5 = 3.79 Å

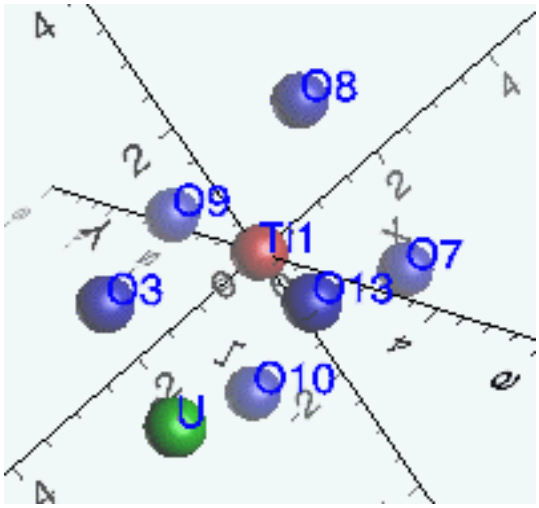

Ti(1) Distorted Octahedron
Bond Angle O3-Ti5-O13= 74.2°
Fixed Bond Lengths:
Ti1-O3 = 2.19 Å
Ti1-O13 = 1.84 Å
U-O3 = 2.40 Å
U-O13 = 2.40 Å
Resultant Radial Distance:
U-Ti1 = 3.61 Å

Supplemental Figure 13. Molecular modeling simulations of sorbed U on two distorted Ti octahedra called Ti(1, top image) and T(5, bottom image). The images support the existence of bonds that produce physically realistic U-Ti radial distances of ~3.6 Å and 3.79 Å.